SPECTRAL ELEMENT MODELING AND ANALYSIS OF AN AXIALLY MOVING THERMOELASTIC BEAM-PLATE

Kyungsoo Kwon and Usik Lee

SPECTRAL ELEMENT MODELING AND ANALYSIS OF AN AXIALLY MOVING THERMOELASTIC BEAM-PLATE

KYUNGSOO KWON AND USIK LEE

Axially moving thin-walled structures exposed to sudden external thermal loads may experience severe vibrations. For accurate predictions of the thermally induced vibrations, this paper develops a spectral element model for the axially moving beam-plates subjected to sudden external thermal loads. The spectral element model is formulated from the frequency-dependent dynamic shape functions which satisfy the governing equations in the frequency domain. Thus, when compared with the conventional finite element model in which simple polynomials are used as the shape functions, the spectral element model provides exact solutions by treating a whole uniform structure member as a single finite element, regardless of its length. Numerical studies are conducted to evaluate the present spectral element model and also to investigate the dynamic characteristics of an axially moving beam-plate subjected to a sudden thermal load on its upper surface.

1. Introduction

A sudden thermal load applied to a structure may induce rapid movements in that structure, causing it to vibrate. These thermally induced vibrations may be encountered, for example, in high-speed modern aircraft subjected to aerodynamic heating, nuclear reactors in extremely high temperature and temperature gradient environments, high-speed propulsion units, and galvanized steel strips passing through a hot zinc tank.

The thermally induced vibration of a beam subjected to a suddenly applied heat flux distributed along its span was studied in [Boley 1956]. Since then many studies have been conducted for various thermoelastic structures such as beams [Boley and Barber 1957; Yu 1969; Manolis and Beskos 1980; Massalas and Kalpakidis 1984; Eslami and Vahedi 1989; Kidawa-Kukla 1997], laminated beams [Al-Huniti 2004], plates [Boley 1956; Kozlov 1972; Takeuti and Furukawa 1981; Massalas et al. 1982; Trajkovski and Čukić 1999; Verma 2001; Arafat et al. 2003; Al-Huniti 2004], laminated plates [Chandrashekhara and Tenneti 1994; Mukherjee and Sinha

1996], panels [Sharma 2001; Oguamanam et al. 2004], cylinders [Takeuti et al. 1983], and so forth. [Lee 1985] conducted thermoelastic damping analysis for the beams, plates and shells undergoing flexural vibration, and [Kinra and Milligan 1994] considered thermoelastic damping for beams. [Tauchert 1991] presented an extensive review on the subject of thermally induced vibrations of plates, and [Thornton 1992] made a survey of the literature on thermal structures, mostly focusing on aerospace applications. To eliminate the paradox of infinite velocity of heat propagation in the classical theory of thermoelasticity [Biot 1956], some researchers such as [Lord and Shulman 1967] developed the generalized theory of thermoelasticity by introducing thermal relaxation times. However, as the thermal relaxation effect is very small at high temperatures [Lord and Shulman 1967], the classical theory of thermoelasticity will be adopted in this study. In the existing literatures, various solution techniques have been used: they include the Green function method [Kidawa-Kukla 1997], integral transformation method [Massalas et al. 1982; Trajkovski and Čukić 1999; Sharma 2001; Al-Huniti 2004], finite element method [Eslami and Vahedi 1989; Chandrashekhara and Tenneti 1994; Mukherjee and Sinha 1996; Oguamanam et al. 2004], and the modal analysis method [Lee 1985].

Existing studies on thermally induced vibration have focused mostly on stationary (not axially moving) thermoelastic structures. Recently, Al-Huniti [2004] considered the dynamics of a stationary laminated beam under the effect of a moving heat source. However, to our best knowledge, the dynamics of axially moving thermoelastic structures such as the galvanized steel strips passing through a hot zinc tank has not been investigated. Furthermore, the spectral element method (SEM) has not been applied to such axially moving thermoelastic structures. The SEM is an element method, like the finite element method (FEM). The fundamental differences from FEM are:

(1) The SEM uses a spectral element matrix (*exact* dynamic stiffness matrix), which is formulated in the frequency domain by using the dynamic (frequency-dependent) shape functions exactly solved from governing equations.

(2) The FFT algorithm is used to efficiently reconstruct the time domain response from the frequency domain solution. Because no approximation or assumption is made in the course of spectral element formulation, SEM indeed provides exact solutions and thus it is well recognized as an *exact* solution method [Lee and Leung 2000; Lee 2004].

In this paper we develop an SEM for an axially moving thermoelastic beam-plate and conduct a spectral element analysis to investigate the dynamic behavior of an axially moving beam-plate subjected to a sudden temperature change on its surface.
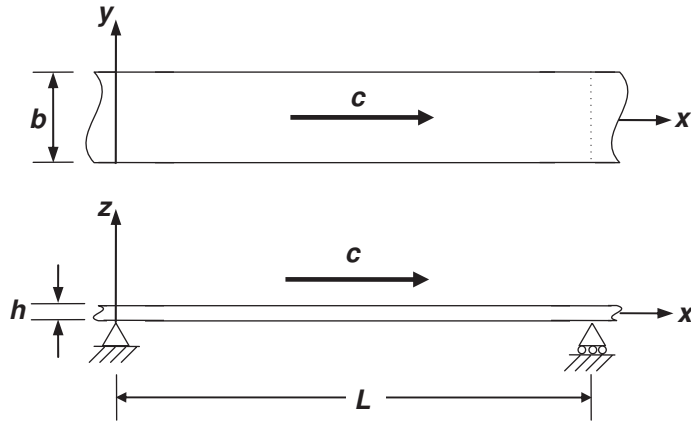
Figure 1. Geometry of an axially moving beam-plate.

2. Derivation of the governing equations

2A. *Equations of motion.* Consider a thin beam-plate moving in the x (axial) direction at speed c, as shown in Figure 1. The beam-plate has thickness h and width b. The material properties of the beam-plate are given by Young's modulus E and Poisson's ratio v. Assume that the beam-plate has a small amplitude vibration and that its displacements don't vary along the width direction as the word 'beam-plate' implies.

Using Kirchhoff's hypothesis, one can write the displacements as

$$W(x, t) = w(x, t),$$
$$U(x, z, t) = u(x, t) - zw'(x, t), \tag{1}$$

where $w(x, t)$ is the displacement of the midplane of the beam-plate in the z direction, $u(x, t)$ the displacement in the x direction, z is the transverse distance from the midplane to the point of interest on the cross-section of the beam-plate, and the prime denotes the derivative with respective to x. From (1), the strain in the x direction can be readily obtained as

$$\varepsilon_{xx} = U'(x, z, t) = u'(x, t) - zw''(x, t). \tag{2}$$

The stress in the x direction, taking into account the thermal stress, is given by [Ugral 1999]

$$\sigma_{xx} = \frac{E}{1 - v^2} \varepsilon_{xx} - \frac{E\alpha}{1 - v} \Delta T(x, z, t), \tag{3}$$

where $\Delta T(x, z, t)$ is the difference between the absolute temperature $T(x, z, t)$ and the reference, stress-free absolute temperature T_0 as

$$\Delta T(x, z, t) = T(x, z, t) - T_0.$$

Using (2) and (3) we can derive the strain energy P as

$$P = \frac{1}{2} \int_0^L \int_{-h/2}^{h/2} \sigma_{xx} \varepsilon_{xx} b \, dz \, dx = \frac{1}{2} \int_0^L (D w''^2 + \overline{EA} u'^2 + M_T w'' - N_T u') \, dx, \quad (4)$$

where L is the span between two simple supports (see Figure 1), A is the cross-sectional area of the beam-plate, and the following definitions are used:

$$D = \frac{EI}{(1 - v^2)}, \qquad I = \frac{bh^3}{12}, \qquad \overline{EA} = \frac{EA}{1 - v^2}. \quad (5)$$

In Equation (4), M_T and N_T are the thermal moment and thermal (axial) force, defined by

$$M_T(x, t) = \frac{E\alpha b}{1 - v} \int_{-h/2}^{h/2} \Delta T(x, z, t) z \, dz,$$

$$N_T(x, t) = \frac{E\alpha b}{1 - v} \int_{-h/2}^{h/2} \Delta T(x, z, t) \, dz. \quad (6)$$

Similarly, by using (1), the kinetic energy K can be derived as

$$K = \frac{\rho}{2} \int_0^L \int_{-h/2}^{h/2} \left((c + \dot{U})^2 + (\dot{W} + c W')^2 \right) b \, dz \, dx$$

$$= \frac{\rho}{2} \int_0^L \left(A(c + \dot{u})^2 + A(\dot{w} + c w')^2 + I \dot{w}'^2 \right) dx. \quad (7)$$

Finally, the virtual work is given by

$$\delta W = \int_0^L \left(p_x(x, t) \delta u(x, t) + p_z(x, t) \delta w(x, t) \right) dx$$
$$+ M_1(t) \delta \phi_1(t) + M_2(t) \delta \phi_2(t) + V(t)_1 \delta w_1(t)$$
$$+ V_2(t) \delta w_2(t) + N_1(t) \delta u_1(t) + N_2(t) \delta u_2(t), \quad (8)$$

where $p_x(x, t)$ and $p_z(x, t)$ are distributed loads acting on the beam-plate in the x and z directions. M_i, V_i and N_i ($i = 1, 2$) represent the boundary moments, transverse shear forces and axial forces applied at $x = 0$ and L, respectively. The transverse displacement, axial displacement and slope ($\phi = \partial w / \partial x$) at boundaries

are defined by

$$w_1(t) = w(0, t), \qquad w_2(t) = w(L, t),$$
$$\phi_1(t) = w'(0, t), \qquad \phi_2(t) = w'(L, t),$$
$$u_1(t) = u(0, t), \qquad u_2(t) = u(L, t).$$

The equations of motion and the relevant boundary conditions of the beam-plate can be derived from Hamilton's principle:

$$\int_{t_1}^{t_2} (\delta K - \delta P + \delta W) \, dt = 0.$$

Substituting (4), (7), and (8) into this equality and integrating by parts yields

$$\int_{t_1}^{t_2} \int_0^L \left(-Dw'''' - \rho A c^2 w'' - 2\rho A c \dot{w}' - \rho A \ddot{w} + \rho I \ddot{w}'' - \tfrac{1}{2} M_T'' + p_z \right) \delta w \, dx \, dt$$

$$+ \int_{t_1}^{t_2} \int_0^L \left(-\rho A \ddot{u} + \overline{EA} u'' - \tfrac{1}{2} N_T' + p_x \right) \delta u \, dx \, dt$$

$$+ \int_{t_1}^{t_2} \left(-M(x, t)\delta\phi \big|_0^L + M_1 \delta\phi_1 + M_2 \delta\phi_2 - V(x, t)\delta w \big|_0^L + V_1 \delta w_1 + V_2 \delta w_2 \right.$$

$$\left. -N(x, t)\delta u \big|_0^L + N_1 \delta u_1 + N_2 \delta u_2 \right) dt = 0, \quad (9)$$

where the limits 0 and L refer to the variable x, and where

$$M(x, t) = Dw'' + \tfrac{1}{2} M_T,$$
$$V(x, t) = -Dw''' - \rho h c^2 w' - \tfrac{1}{2} M_T' - \rho A c \dot{w} + \rho I \ddot{w}', \qquad (10)$$
$$N(x, t) = \overline{EA} u' - \tfrac{1}{2} N_T.$$

From the first two integrals in (9) we obtain the equations of motion:

$$\overline{EA} u'' - \rho A \ddot{u} = -p_x(x, t) + \tfrac{1}{2} N_T', \qquad (11)$$

$$Dw'''' + \rho A c^2 w'' + 2\rho A c \dot{w}' - \rho I \ddot{w}'' + \rho A \ddot{w} = \quad p_z(x, t) - \tfrac{1}{2} M_T''. \qquad (12)$$

The boundary conditions can be obtained from the last integral of (9) as

$$M(0, t) = -M_1(t) \quad \text{or} \quad \phi(0, t) = \phi_1(t),$$
$$M(L, t) = M_2(t) \quad \text{or} \quad \phi(L, t) = \phi_1(t),$$
$$V(0, t) = -V_1(t) \quad \text{or} \quad w(0, t) = w_1(t),$$
$$V(L, t) = V_2(t) \quad \text{or} \quad w(L, t) = w_2(t), \qquad (13)$$
$$N(0, t) = -N_1(t) \quad \text{or} \quad u(0, t) = u_1(t),$$
$$N(L, t) = N_2(t) \quad \text{or} \quad u(L, t) = u_2(t).$$

2B. ***Heat conduction equation.*** The temperature field $T(x, z, t)$ or $\Delta T(x, z, t)$ is governed by the heat conduction equation. The heat conduction equation can be derived from the law of energy conservation as [Lee 1985; Özisik 1993]

$$-q'_x - q'_z - \frac{T_0 \alpha E}{1 - 2\nu} \frac{\partial e}{\partial t} = \rho c_p \frac{\partial T}{\partial t}, \tag{14}$$

where α is the coefficient of thermal expansion and c_p is the specific heat at constant strain. The first two terms in the left of Equation (14) represent the net energy inflow and q_x and q_z are the heat fluxes per unit area in the x and z directions, respectively, defined by

$$\begin{aligned}
q_x(x, z, t) &= -kT'(x, z, t) + \rho c_p c \Delta T(x, z, t), \\
q_z(x, z, t) &= -kT^\circ(x, z, t),
\end{aligned} \tag{15}$$

where k is the thermal conductivity of the medium. The circle ($^\circ$) symbol denotes the derivative with respective to z and this notation will be used throughout. Notice that the effect of the moving speed c is taken into account in the heat flux q_x [Özisik 1993; Beck and McMasters 2004]. The term on the right in Equation (14) represents the energy stored in the structure. The third term on the left represents the rate of thermal energy generation due to elastic deformation, where $e(x, z, t)$ is the dilatation defined by [Lee 1985; Ugral 1999]

$$e = \varepsilon_{xx} + \varepsilon_{yy} + \varepsilon_{zz} \cong \left(\frac{1 - 2\nu}{1 - \nu} \right) (u' - zw'') + \left(\frac{1 + \nu}{1 - \nu} \right) \alpha \Delta T \cong \left(\frac{1 + \nu}{1 - \nu} \right) \alpha \Delta T, \tag{16}$$

where ε_{xx}, ε_{yy}, ε_{zz} are the normal strains in the x, y, z directions. In (16), the strain ε_{yy} is neglected because we are considering a beam-plate. The dilatation due to the pure elastic deformation is also neglected in the last expression of (16) because its effect on the temperature change will be a small, secondary effect.

Substituting (15) and (16) in (14) gives the heat conduction equation as

$$-k(T'' + T^{\circ\circ}) + \rho c_p c T' + (T_0 \alpha^2 E_\nu + \rho c_p) \dot{T} \cong 0, \tag{17}$$

where

$$E_\nu = \frac{1 + \nu}{(1 - 2\nu)(1 - \nu)} E. \tag{18}$$

In deriving the heat conduction equation, we have implicitly assumed that the heating of the plate will not exceed the limit where the material's thermal and mechanical properties become temperature-dependent. In addition, we will assume that the beam-plate is subject to the thermal loads applied only on its top or bottom surface and that the thermal loads do not vary along the width direction, y. Because of the geometry of beam-plate and the y-axis independence of thermal loads, the instantaneous temperature variation due to the sudden temperature change on the

top or bottom surface of beam-plate will be more significant in the thickness direction than in the in-plane direction. Accordingly, one may assume the temperature as the function of z and t to simplify (17) as follows:

$$kT^{\circ\circ} - \left(T_0 \alpha^2 E_v + \rho c_p\right)\dot{T} = 0. \tag{19}$$

Once the proper thermal boundary conditions are specified for a given problem, one can readily solve Equation (18) for $T(z, t)$ and then apply the solution to Equation (11) to investigate the thermal-induced vibration of a beam-plate. Notice that, because the temperature will be assumed in this study as the function of z and t only, the thermal moment M_T and thermal force N_T defined by Equation (6) will be functions of t only. In this case, the last terms in (11) will vanish and the thermal loads will affect the vibration of beam-plate through the boundary conditions, which can be guessed from Equations (10) and (13).

3. Spectral element formulation

3A. *Brief review of DFT theory.* (For more details, see for instance [Newland 1993].) In discrete Fourier transform (DFT) theory, a periodic function of time $x(t)$ with period T can be always expressed by the Fourier series as

$$x(t) = \sum_{n=-\infty}^{\infty} X_n e^{i\omega_n t}, \tag{20}$$

where $i = \sqrt{-1}$, $\omega_n = n(2\pi/T) = n\omega_1$ are the discrete frequencies, and X_n are constant Fourier (or spectral) components given by

$$X_n = \frac{1}{T} \int_0^T x(t) e^{-i\omega_n t} \, dt \quad (n = 0, 1, 2, \ldots, \infty). \tag{21}$$

Equations (20) and (21) are the continuous Fourier transforms pair for a periodic function.

Although $x(t)$ is a continuous function of time t, it is often the case that only sampled values of the function are available, in the form of a discrete time series $\{x(t_r)\}$. If N is the number of samples, all equally spaced with a time interval $\Delta = T/N$, the discrete time series are given by $x_r = x(t_r)$, where $t_r = r\Delta$ and $r = 0, 1, 2, \ldots, N-1$. The integral in Equation (21) can be replaced with the summation as follows:

$$X_n = \sum_{r=0}^{N-1} x(t_r) e^{-i\omega_n t_r} \quad (n = 0, 1, 2, \ldots, N-1), \tag{22}$$

which is the DFT of the discrete time series $\{x_r\}$. Any typical value x_r of the series $\{x_r\}$ can be obtained from the synthesis equation

$$x(t_r) = \frac{1}{N} \sum_{n=0}^{N-1} X_n e^{i\omega_n t_r} \quad (r = 0, 1, 2, \ldots, N-1), \tag{23}$$

which is the inverse discrete Fourier transform (IDFT). Thus Equations (22) and (23) represent the DFT-IDFT pair. Although (22) is an approximation of (20), it allows all discrete time series $\{x_r\}$ to be regained *exactly* [Newland 1993]. The Fourier components X_n in (23) can normally be arranged as

$$X_{N-n} = X_n^* \quad (n = 0, 1, 2, \ldots, N/2),$$

where * denotes complex conjugation. $X_{N/2}$ corresponds to the highest frequency $\omega_{N/2} = (N/2)\omega_1$, the Nyquist frequency.

The fast Fourier transforms (FFT) is an ingenious computer algorithm that performs the synthesis analysis extremely efficiently, in time logarithmic rather than linear in N. While the FFT-based spectral analysis uses a computer, it is not a numerical method in the usual sense, because the analytical descriptions of Equations (22) and (23) are retained.

3B. *Formulation of the spectral element matrix.* Based on DFT theory, assume the solutions of Equation (11) in spectral form are

$$u(x, t) = \sum_{n=0}^{N-1} U_n(x) e^{i\omega_n t}, \qquad w(x, t) = \sum_{n=0}^{N-1} W_n(x) e^{i\omega_n t}, \tag{24}$$

where $U_n(x)$ and $W_n(x)$, for $n = 0, 1, \ldots, N-1$, are the spectral components of the dynamic responses $u(x, t)$ and $w(x, t)$. The accuracy of dynamic responses may depend on how many spectral components are taken into account in the FFT-based spectral analysis, for a chosen time window T. Similarly, one can express the external loads and thermal loads in the spectral forms as

$$p_x(x, t) = \sum_{n=0}^{N-1} P_{xn}(x) e^{i\omega_n t}, \qquad p_z(x, t) = \sum_{n=0}^{N-1} P_{zn}(x) e^{i\omega_n t},$$

$$N_T(t) = \sum_{n=0}^{N-1} N_{Tn} e^{i\omega_n t}, \qquad M_T(t) = \sum_{n=0}^{N-1} M_{Tn} e^{i\omega_n t}, \tag{25}$$

where $P_{xn}(x)$, $P_{zn}(x)$, $N_{Tn}(x)$ and $M_{Tn}(x)$, for $n = 0, 1, \ldots, N-1$, are the spectral components of $p_x(x, t)$, $p_y(x, t)$, $N_T(t)$, and $M_T(t)$. The spectral components M_{Tn} and N_{Tn} in Equation (25) are constant, rather than functions of x, because the temperature is assumed to vary only in the thickness (z) direction.

Substituting (24) and (25) into (11), we get

$$\overline{EA}U_n'' + \rho A\omega_n^2 U_n = F_{xn},$$
$$DW''''_n + (\rho Ac^2 + \rho I\omega_n^2)W_n'' + 2i\rho Ac\omega_n W_n' - \rho A\omega_n^2 W_n = F_{zn}, \tag{26}$$

where

$$F_{xn}(x) = -P_{xn} + \tfrac{1}{2}N'_{Tn} = -P_{xn}, \qquad F_{zn}(x) = P_{zn} - \tfrac{1}{2}M''_{Tn} = P_{zn}. \tag{27}$$

Here the thermal force and moment terms do not appear because temperature is assumed to vary only in the thickness direction. In a similar way, the resultant moment, transverse shear force and axial force defined in (10) can be also expressed in spectral form as

$$N_n(x) = \overline{EA}U_n' - \tfrac{1}{2}N_{Tn},$$
$$V_n(x) = -DW_n''' - (\rho Ac^2 + \rho I\omega_n^2)W_n' - i\rho Ac\omega_n W_n, \tag{28}$$
$$M_n(x) = DW_n'' + \tfrac{1}{2}M_{Tn},$$

where $N_n(x)$, $V_n(x)$ and $M_n(x)$ are the spectral components of $N(x,t)$, $V(x,t)$ and $M(x,t)$, respectively.

The spectral element formulation begins with the governing equations without external forces [Lee and Leung 2000; Lee 2004]. Therefore, the homogeneous form of governing equations can be deduced from (26) as

$$\overline{EA}U_n'' + \rho A\omega_n^2 U_n = 0,$$
$$DW''''_n + (\rho Ac^2 + \rho I\omega_n^2)W_n'' + 2i\rho Ac\omega_n W_n' - \rho A\omega_n^2 W_n = 0. \tag{29}$$

The general solutions of (29) can be assumed to be

$$U_n(x) = A_n e^{\kappa_n x}, \qquad W_n(x) = B_n e^{\lambda_n x},$$

where κ_n and λ_n are the wavenumbers for the axial and transverse vibration mode, respectively. Substituting these equalities into (29) yields the dispersion relations

$$\overline{EA}k_n^2 + \rho A\omega_n^2 = 0,$$
$$D\lambda_n^4 + (\rho Ac^2 + \rho I\omega_n^2)\lambda_n^2 + 2i\rho Ac\omega_n\lambda_n - \rho A\omega_n^2 = 0.$$

From this, two wavenumbers k_{nr} ($r = 1, 2$) can be obtained for axial vibration modes and four wavenumbers λ_{nr} ($r = 1, 2, 3, 4$) for the transverse vibration modes. By using the wavenumbers thus computed, the general solutions of the dispersion relations can expressed in summation form as

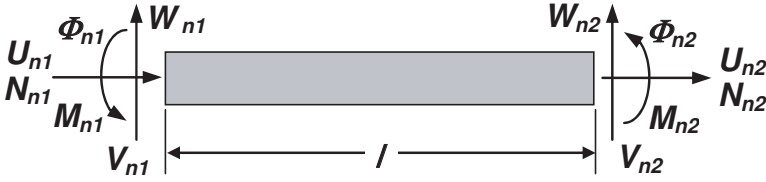$$U_n(x) = \sum_{r=1}^{2} A_{nr} e^{k_{nr}x}, \qquad W_n(x) = \sum_{r=1}^{4} B_{nr} e^{\lambda_{nr}x},$$

Figure 2. Sign convention for finite beam-plate element.

or in matrix-vector multiplication form as

$$
\begin{aligned}
U_n(x) &= \big[\boldsymbol{E}_{Un}(x;\omega_n)\big]\{\boldsymbol{C}_n\}, \\
W_n(x) &= \big[\boldsymbol{E}_{Wn}(x;\omega_n)\big]\{\boldsymbol{C}_n\},
\end{aligned}
\tag{30}
$$

where

$$
\big[\boldsymbol{E}_{Un}(x;\omega_n)\big] = \big[e^{k_{n1}x}\ \ 0\ \ 0\ \ e^{k_{n2}x}\ \ 0\ \ 0\big],
$$

$$
\big[\boldsymbol{E}_{Wn}(x;\omega_n)\big] = \big[0\ \ e^{\lambda_{n1}x}\ \ e^{\lambda_{n2}x}\ \ 0\ \ e^{\lambda_{n3}x}\ \ e^{\lambda_{n4}x}\big],
$$

$$
\{\boldsymbol{C}_n\} = \big\{A_{n1}\ \ B_{n1}\ \ B_{n2}\ \ A_{n2}\ \ B_{n3}\ \ B_{n4}\big\}^T.
$$

The constant vector $\{\boldsymbol{C}_n\}$ will be determined by the boundary conditions.

Now consider a finite beam-plate element of length l as shown in Figure 2. The corresponding spectral components of the nodal degree of freedom (DOF) are defined by

$$
\begin{array}{lll}
U_{n1} = U_{n1}(0), & W_{n1} = W_{n1}(0), & \Phi_{n1} = W'_{n1}(0), \\
U_{n2} = U_{n2}(l), & W_{n2} = W_{n2}(l), & \Phi_{n2} = W'_{n2}(l).
\end{array}
$$

Applying these values to Equation (30) yields a relationship between the spectral nodal DOF vector $\{\boldsymbol{d}_n\}$ and the constant vector $\{\boldsymbol{C}_n\}$:

$$
\{\boldsymbol{d}_n\} = \big[\boldsymbol{X}_n(\omega_n)\big]\{\boldsymbol{C}_n\},
\tag{31}
$$

where $\{\boldsymbol{d}_n\} = \big\{U_{n1}\ \ W_{n1}\ \ \Phi_{n1}\ \ U_{n2}\ \ W_{n2}\ \ \Phi_{n2}\big\}^T$ and

$$
[\boldsymbol{X}_n] =
\begin{bmatrix}
1 & 0 & 0 & 1 & 0 & 0 \\
0 & 1 & 1 & 0 & 1 & 1 \\
0 & \lambda_{n1} & \lambda_{n2} & 0 & \lambda_{n3} & \lambda_{n4} \\
e^{k_{n1}l} & 0 & 0 & e^{k_{n2}l} & 0 & 0 \\
0 & e^{\lambda_{n1}l} & e^{\lambda_{n2}l} & 0 & e^{\lambda_{n3}l} & e^{\lambda_{n4}l} \\
0 & \lambda_{n1}e^{\lambda_{n1}l} & \lambda_{n2}e^{\lambda_{n2}l} & 0 & \lambda_{n3}e^{\lambda_{n3}l} & \lambda_{n4}e^{\lambda_{n4}l}
\end{bmatrix}.
$$

One can use (31) to eliminate the constant vector $\{C_n\}$ from Equation (30), obtaining

$$U_n(x) = [E_{Un}][X_n]^{-1}\{d_n\} \equiv [N_{Un}(x; \omega_n)]\{d_n\},$$
$$W_n(x) = [E_{Wn}][X_n]^{-1}\{d_n\} \equiv [N_{Wn}(x; \omega_n)]\{d_n\}, \tag{32}$$

where $[N_{Un}]$ and $[N_{Wn}]$ are the dynamic (frequency-dependent) shape function matrices.

In the following, the well-known variational approach [Reddy 2002] is used to formulate the spectral element matrix by using the displacement fields given by Equation (32) and the temperature field given in the next section. The weak form statements of the governing equations (26) are

$$\int_0^l \left(\overline{EA}U_n'' + \rho A\omega_n^2 U_n + P_{xn}\right)\delta U_n\, dx = 0,$$

$$\int_0^l \left(DW''''_n + (\rho Ac^2 + \rho I\omega_n^2)W_n'' + 2i\rho Ac\omega_n W_n' - \rho A\omega_n^2 W_n - P_{zn}\right)\delta W_n\, dx = 0.$$

Substituting the loading terms from (27) into these equalities and integrating by parts yields

$$\int_0^l \left(\overline{EA}\,U_n'\,\delta U_n' - \rho A\omega_n^2 U_n\,\delta U_n\right)dx - \int_0^l P_{xn}\,\delta U_n\, dx - \tfrac{1}{2}N_{Tn}\,\delta U_n\big|_0^l - N_n\,\delta U_n\big|_0^l = 0,$$

$$\int_0^l \left(DW_n''\,\delta W_n'' - (\rho Ac^2 + \rho I\omega_n^2)W_n'\,\delta W_n' + i\rho Ac\omega_n(W_n'\,\delta W_n - W_n\,\delta W_n')\right.$$
$$\left. - \rho A\omega_n^2 W_n\,\delta W_n\right)dx - \int_0^l P_{zn}\,\delta W_n\, dx + \tfrac{1}{2}M_{Tn}\,\delta W_n'\big|_0^l - V_n\,\delta W_n\big|_0^l - M_n\,\delta W_n'\big|_0^l = 0,$$

where Equation (28) has been used and where, as before, the limits 0 and l refer to the variable x.

Substituting (32) into these two equalities yields

$$\{\delta d_n\}^T\left([S_{Un}]\{d_n\} - \{f_{Un}\}\right) = 0, \qquad \{\delta d_n\}^T\left([S_{Wn}]\{d_n\} - \{f_{Wn}\}\right) = 0, \quad (33)$$

where

$$[S_{Un}] = \int_0^l \left(\overline{EA}[N_{Un}']^T[N_{Un}'] - \rho A\omega_n^2[N_{Un}]^T[N_{Un}]\right)dx,$$

$$[S_{Wn}] = \int_0^l \left(D[N_{Wn}'']^T[N_{Wn}''] - (\rho Ac^2 + \rho I\omega_n^2)[N_{Wn}']^T[N_{Wn}']\right.$$
$$\left. + i\rho Ac\omega_n\left([N_{Wn}]^T[N_{Wn}'] - [N_{Wn}']^T[N_{Wn}]\right) - \rho A\omega_n^2[N_{Wn}]^T[N_{Wn}]\right)dx, \quad (34)$$

$$\{f_{Un}\} = \{N_{1n} \; 0 \; 0 \; N_{2n} \; 0 \; 0\}^T + \int_0^l P_{xn}(x)[N_{Un}]^T dx - \frac{1}{2}N_{Tn}[N_{Un}(l) - N_{Un}(0)]^T,$$

$$\{f_{Wn}\} = \{0 \; V_{1n} \; M_{1n} \; 0 \; V_{2n} \; M_{2n}\}^T + \int_0^l P_{zn}(x)[N_{Wn}]^T dx$$
$$+ \frac{1}{2}M_{Tn}[N'_{Wn}(l) - N'_{Wn}(0)]^T.$$

The details of the matrices $[S_{Un}]$ and $[S_{Wn}]$ are given in the Appendix.

Since $\{\delta d_n\}$ is arbitrary, the spectral element equation can be deduced from (33):

$$[S_n(\omega)]\{d_n\} = \{f_n\}. \tag{35}$$

Here

$$[S_n(\omega)] = [S_{Un}(\omega)] + [S_{Wn}(\omega)]$$

is the frequency-dependent spectral element matrix and

$$\{f_n\} = \{f_n\}_1 + \{f_n\}_2$$

is the spectral nodal force, where

$$\{f_n\}_1 = \{N_{1n} \; V_{1n} \; M_{1n} \; N_{2n} \; V_{2n} \; M_{2n}\}^T,$$

$$\{f_n\}_2 = \int_0^l P_{xn}(x)[N_{Un}]^T dx + \int_0^l P_{zn}(x)[N_{Wn}]^T dx \tag{36}$$
$$- \frac{1}{2}N_{Tn}[N_{Un}(l) - N_{Un}(0)]^T + \frac{1}{2}M_{Tn}[N'_{Wn}(l) - N'_{Wn}(0)]^T.$$

All spectral elements can be assembled in a completely analogous way to that used in the conventional FEM. Assembling all spectral elements represented by (35) and then applying appropriate boundary conditions yields a global system equation in the form

$$[S_n^G(\omega)]\{d_n^G\} = \{f_n^G\}.$$

The natural frequencies ω_{NAT} can be computed from the condition that the determinant of global spectral stiffness matrix $[S_n^G]$ should vanish at natural frequencies:

$$\det[S_n^G(\omega_{\text{NAT}})] = 0.$$

3C. *Temperature in the frequency domain.* The approximate temperature field is governed by Equation (18) and the thermal boundary conditions specified on the upper and lower surfaces of the beam-plate. As done in the preceding section for the displacements field, the temperature field can be also represented in the spectral form as

$$T(z, t) = \sum_{n=0}^{N-1} T_n(z)e^{i\omega_n t},$$

where T_n are the spectral components of temperature field $T(z,t)$. Substituting this equality into the heat conduction equation (18) yields

$$T_n^{\circ\circ} - i\omega_n\beta^2 T_n = 0, \tag{37}$$

where

$$\beta^2 = \frac{1}{k}\left(T_0\alpha^2 E\eta + \rho c_p\right).$$

The general solution of Equation (37) can be readily obtained as

$$T_n(z) = B_{n1}e^{-\tau_n z} + B_{n2}e^{\tau_n z}, \tag{38}$$

where

$$\tau_n = \beta\sqrt{i\omega_n}\beta = (1+i)\beta\sqrt{\frac{\omega_n}{2}}. \tag{39}$$

The constants B_{n1} and B_{n2} are determined by the thermal boundary conditions specified on the upper and lower surfaces of beam-plate. Once the spectral components of temperature T are computed from (38), the corresponding spectral components of thermal moment M_T and thermal force N_T in (36) can be readily computed from (6) and (25).

4. Numerical results and discussion

As an illustrative example, a beam-plate which is axially moving over two simple supports of distance $L = 2$ m is considered. The beam-plate has thickness $h = 5$ mm, width $b = 0.5$ m, Young's modulus $E = 73$ GPa, Poisson's ratio $\nu = 0.33$, mass density $\rho = 2770$ kg/m³, thermal expansion coefficient $\alpha 23.0 \times 10^{-6}/K$, thermal conductivity $k = 177$ W/mK, and specific heat $c_p = 875$ J/kg· K. As shown in Figure 3, the temperature change is applied only to the middle part of the upper surface, while the remaining parts are allowed to remain at room temperature T_0.

First, to show the high accuracy of the present spectral element model, we compare in Table 1 the natural frequencies obtained for the beam-plate using the
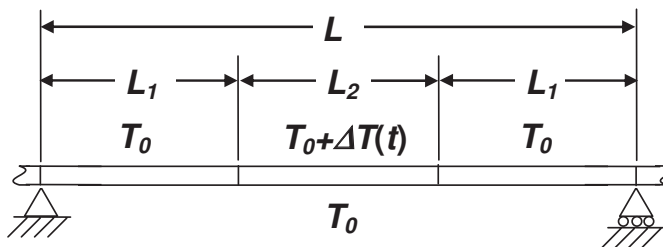

Figure 3. Example problem: thermal boundary conditions on the upper and lower surfaces of the beam-plate which moves axially over two simple supports.

c (m/s)	Method	N	$\omega_1^{(w)}$	$\omega_2^{(w)}$	$\omega_3^{(w)}$	$\omega_4^{(w)}$	$\omega_5^{(w)}$	$\omega_{15}^{(u)}$
	Exact	−	3.083	12.329	27.743	49.321	77.066	679.78
	SEM	1	3.083	12.329	27.742	49.317	77.057	679.78
0		10	3.083	12.331	27.758	49.403	77.371	680.48
	FEM	20	3.083	12.330	27.744	49.327	77.087	679.95
		50	3.083	12.329	27.743	49.322	77.067	679.81
		100	3.083	12.329	27.743	49.322	77.067	679.79
	SEM	1	2.886	12.197	27.626	49.210	76.955	679.78
4		10	2.886	12.198	27.643	49.298	77.274	680.48
	FEM	20	2.886	12.197	27.628	49.220	76.985	679.95
		50	2.886	12.197	27.627	49.215	76.966	679.81
		100	2.886	12.197	27.627	49.215	76.965	679.79
	SEM	1	2.248	11.790	27.277	48.889	76.649	679.78
8		10	2.248	11.792	27.296	48.983	76.982	680.48
	FEM	20	2.248	11.790	27.280	48.899	76.681	679.95
		50	2.248	11.790	27.279	48.893	76.660	679.81
		100	2.248	11.790	27.279	48.893	76.659	679.79
	SEM	1	0.0	11.012	26.631	48.297	76.087	679.78
12.33		10	0.0	11.015	26.654	48.402	76.446	680.48
	FEM	20	0.0	11.012	26.634	48.307	76.120	679.95
		50	0.0	11.012	26.633	48.301	76.098	679.81
		100	0.0	11.012	26.633	48.301	76.097	679.79

Table 1. Natural frequencies (Hz) of a beam-plate obtained by the present SEM, the FEM and the exact theory [Blevins 1979]. N is the number of finite elements used in the analysis, c is the fluid velocity, and the superscripts (w) and (u) stand respectively for the transverse and axial displacement modes.

present spectral element model (SEM), the finite element model (FEM), and the exact theory (only for stationary beam), for various speeds of the beam-plate. The number of finite elements used in the FEM varies from 10 to 100, while only one finite element is used for the SEM. The table shows that the SEM results are almost same as the exact values when $c = 0$, and the FEM values converge to the SEM values when $c \neq 0$ as the number of finite elements used in FEM is increased. This suggests that the present spectral element model is very accurate.

One more thing we can observe from Table 1 is that in general the magnitude of natural frequency (real part of eigenfrequency) decreases as the moving speed of beam-plate is increased. The first natural frequency becomes zero at
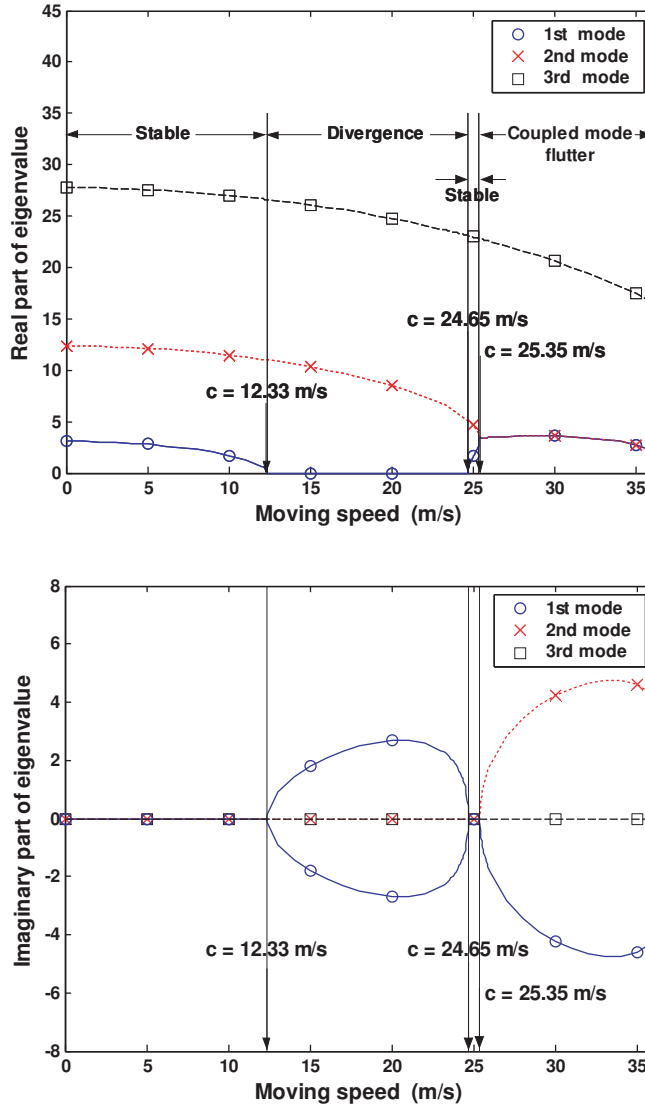
Figure 4. Moving speed dependence of the lowest first three eigenfrequencies of beam-plate.

$c = 12.33$ m/s, which is the divergence speed at which the divergence instability may occur. Figure 4 shows in detail how the eigenfrequency of beam-plate varies as the moving speed of beam-plate is increased. One can see from Figure 4 that the beam-plate will have divergence instability at $c = 12.33$ m/s and coupled-mode flutter instability at $c = 25.35$ m/s.
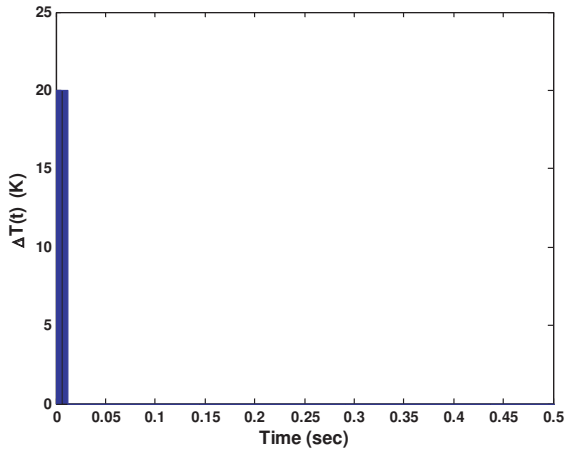
Figure 5. Time history of the thermal load applied on the middle region (L_2) of the upper surface of beam-plate shown in Figure 3.

To investigate the thermally induced vibration of the beam-plate, the temperature on the middle part of the upper surface of the beam-plate is suddenly elevated so that $\Delta T = 20\,\mathrm{K}$ and the elevated temperature is sustained for 0.01 seconds from $t = 0$, as shown in Figure 5. Figure 6 shows the time history of the temperature distribution through the thickness of the beam-plate, and Figure 7
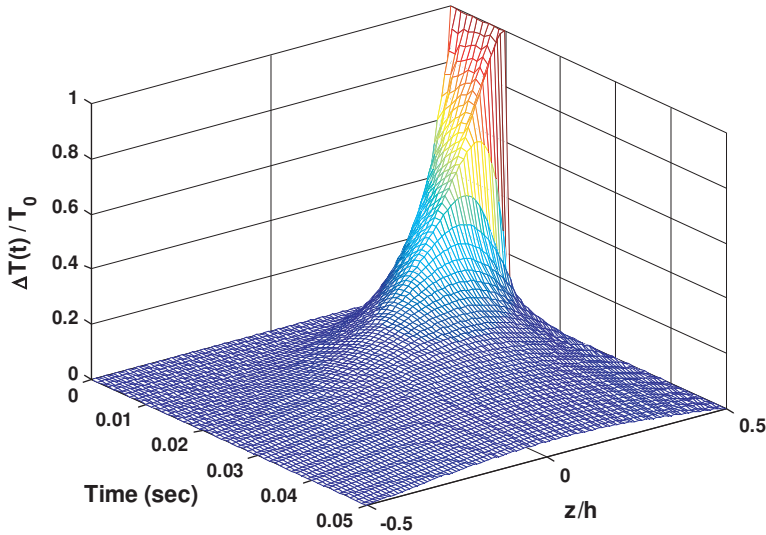
Figure 6. Time history of temperature distribution through the thickness of beam-plate.
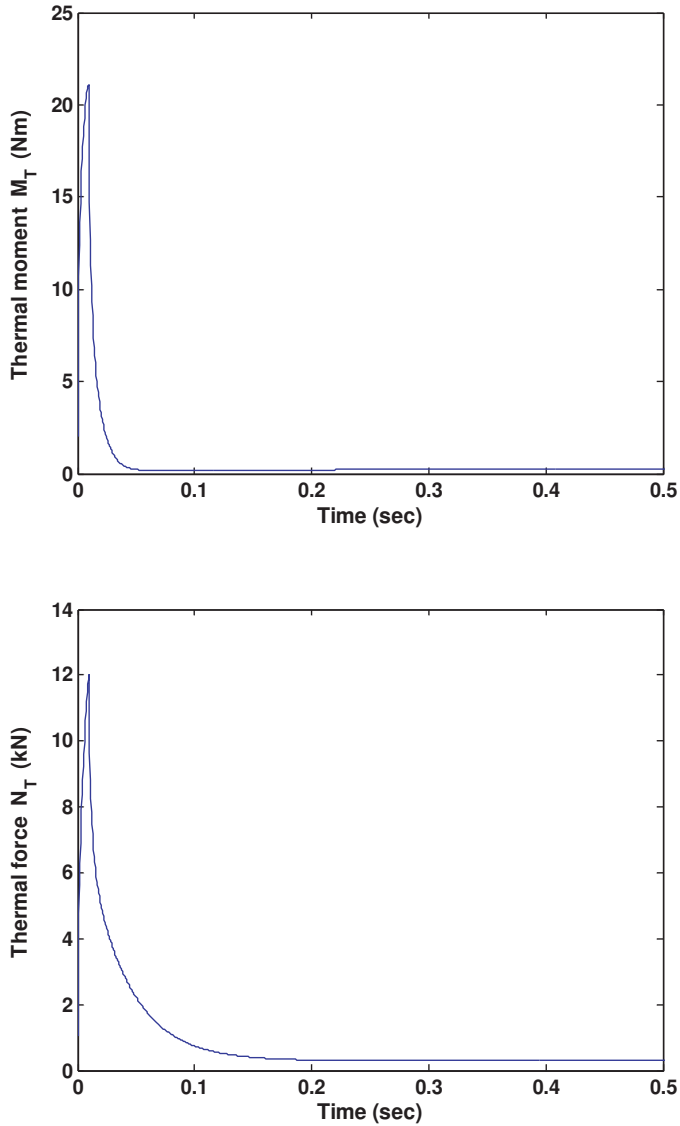
Figure 7. Time histories of the thermal moment M_T and thermal force N_T in the region $L_1 \leq x \leq (L - L_2)$.

shows the corresponding thermal moment M_T and thermal force N_T in the region $L_1 \leq x \leq \quad L - L_2$. Notice that $L_1 = L_3 = 0.8\,\text{m}$ and $L_2 = 0.4\,\text{m}$. Figure 6 shows that the temperature quickly spreads out to become symmetric with respect to the middle plane of the beam-plane. Accordingly the thermal moment M_T disappears after about 0.05 seconds, while the thermal force N_T converges to a small value.
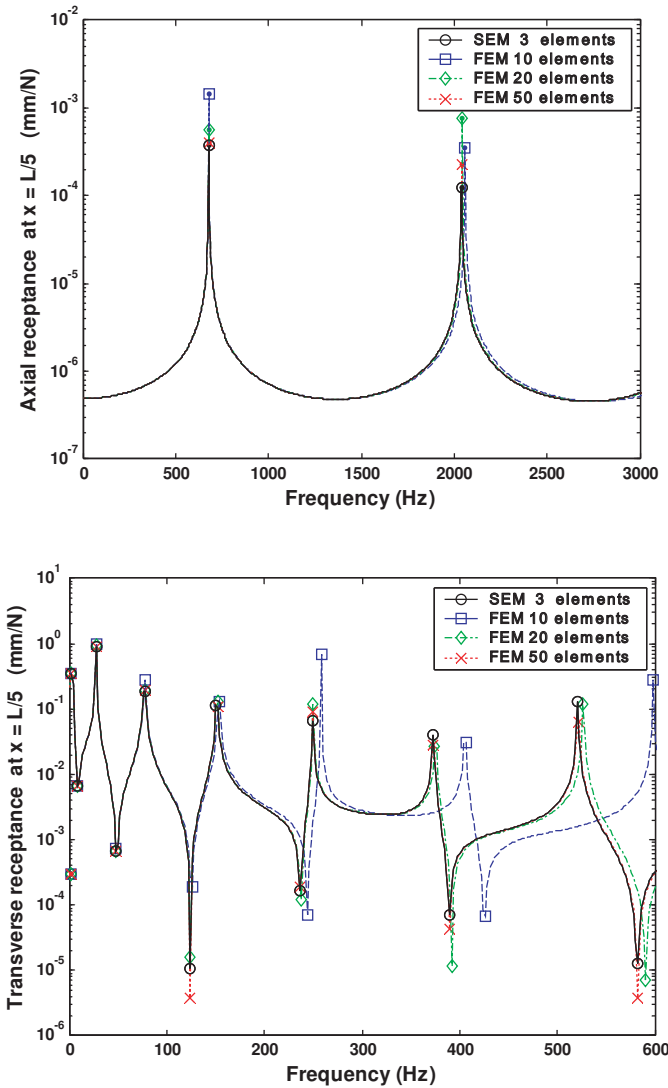
Figure 8. Comparison of the frequency response functions of the axial and transverse displacements obtained by the present SEM and FEM when $c = 4\,\text{m/s}$ and $L_2 = 0.2L$.

Figure 8 compares the frequency response functions obtained by the present SEM and FEM. Similarly Figure 9 compares the corresponding time responses. It is clear from both figures that FEM results converge to SEM results as the number of finite elements used in FEM is increased, which also proves the high accuracy of the present spectral element model. Notice that the minimum number of finite
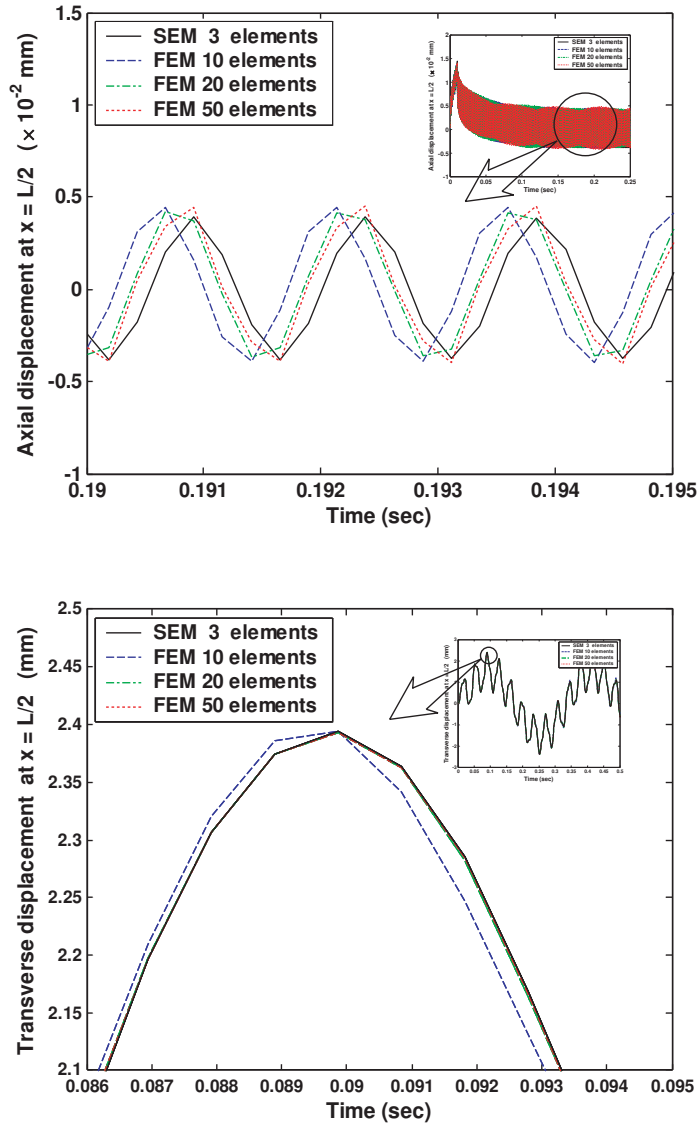
Figure 9. Comparison of the axial and transverse displacements obtained by the present SEM and FEM when $c = 4\,\text{m/s}$ and $L_2 = 0.2L$.

elements used in SEM is three, because the beam-plate has temperature discontinuities at $x = L_1$ and $x = L_1 + L_2$.

Figure 10 shows the time responses of transverse displacement at three different moving speeds of beam-plate. From Figure 10, one can observe that the period of time response increases as the moving speed increases. As previously discussed,
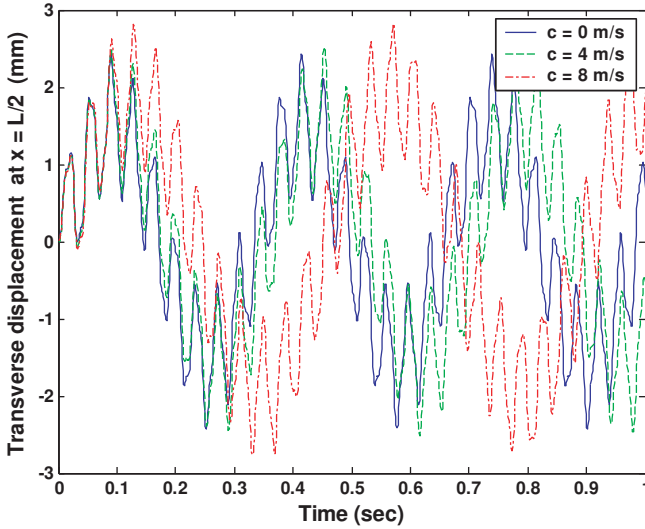
Figure 10. Transverse displacement versus moving speed c when $L_2 = 0.2L$.
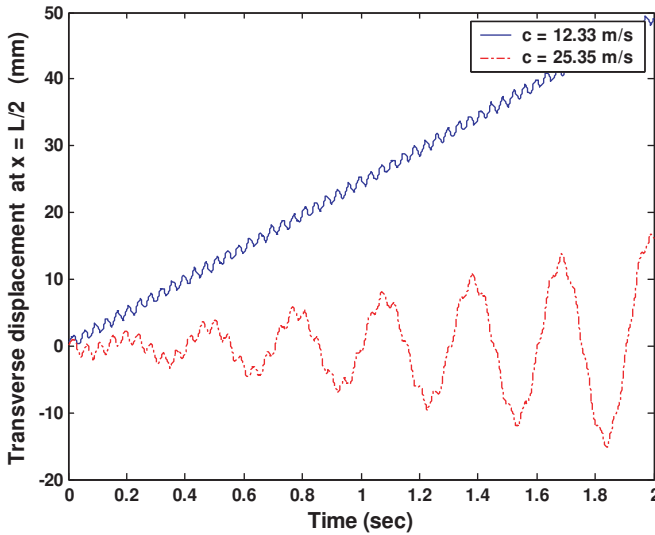

Figure 11. Transverse displacements when $c = 12.33$ m/s (divergence speed) and $c = 25.35$ m/s (flutter speed) when $L_2 = 0.2L$.

this is because the natural frequencies decrease as the moving speed increases. Figure 11 shows the time responses at divergence speed $c = 12.33$ m/s and flutter speed $c = 25.35$ m/s. As expected, the divergence and flutter instabilities indeed occur at the divergence and flutter speeds, respectively.
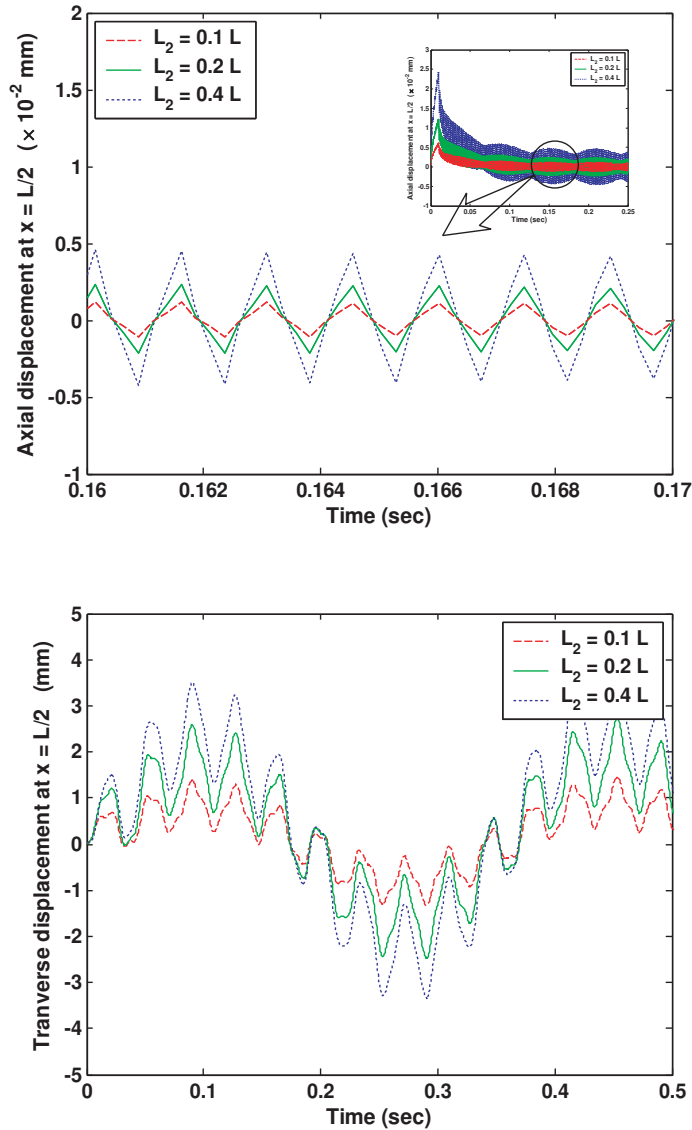
Figure 12. Axial and transverse displacements versus size of L_2 on which thermal load is applied when $c = 4$ m/s.

Figure 12 shows the time responses of axial and transverse displacements depending on the length of middle part (L_2) subjected to the sudden temperature change of Figure 5, when the moving speed of beam-plate is $c = 4$ m/s. The time responses in both axial and transverse displacements tend to increase as the length of middle part becomes larger.
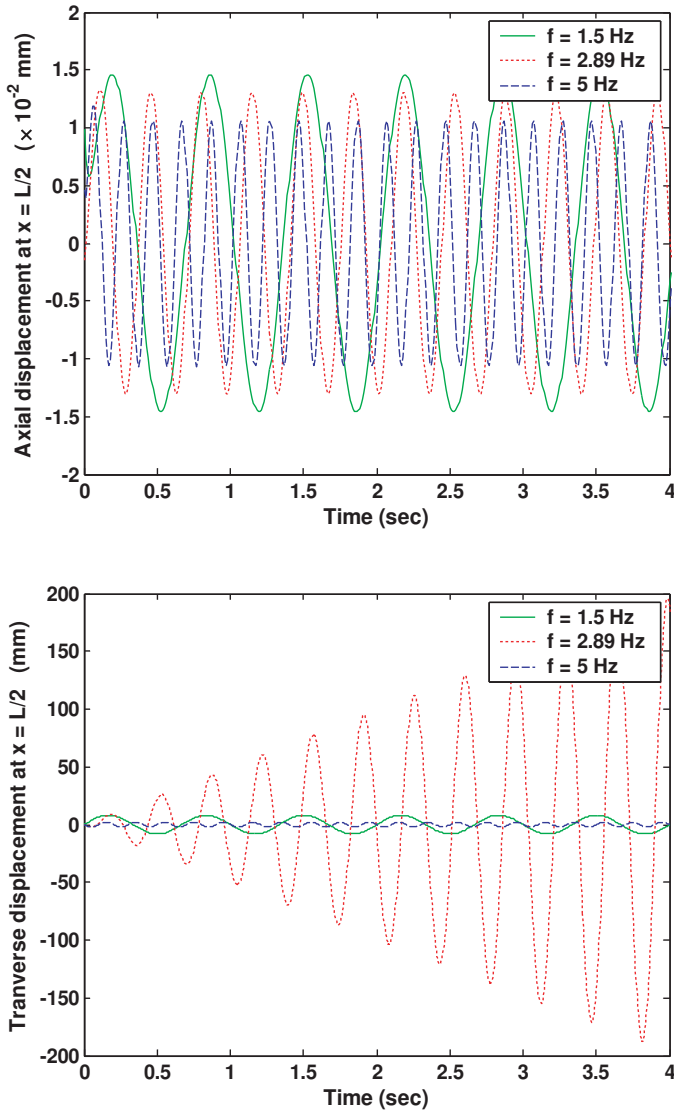
Figure 13. Axial and transverse displacements versus excitation frequency f of the thermal load given by $\Delta T(x, t) = 10 \sin(2\pi f t) + 20(K)$ when $c = 4$ m/s and $L_2 = 0.2L$.

Figure 13 compares the axial and transverse displacements excited by a harmonic thermal load defined by $\Delta T(x, t) = 10 \sin(2\pi f t) + 20(K)$ when $c = 4$ m/s and $L_2 = 0.2L$. It is obvious from Figure 13 that the resonance in transverse vibration mode occurs when the excitation frequency f is close to the first transverse natural frequency 2.886 Hz (see Table 1).
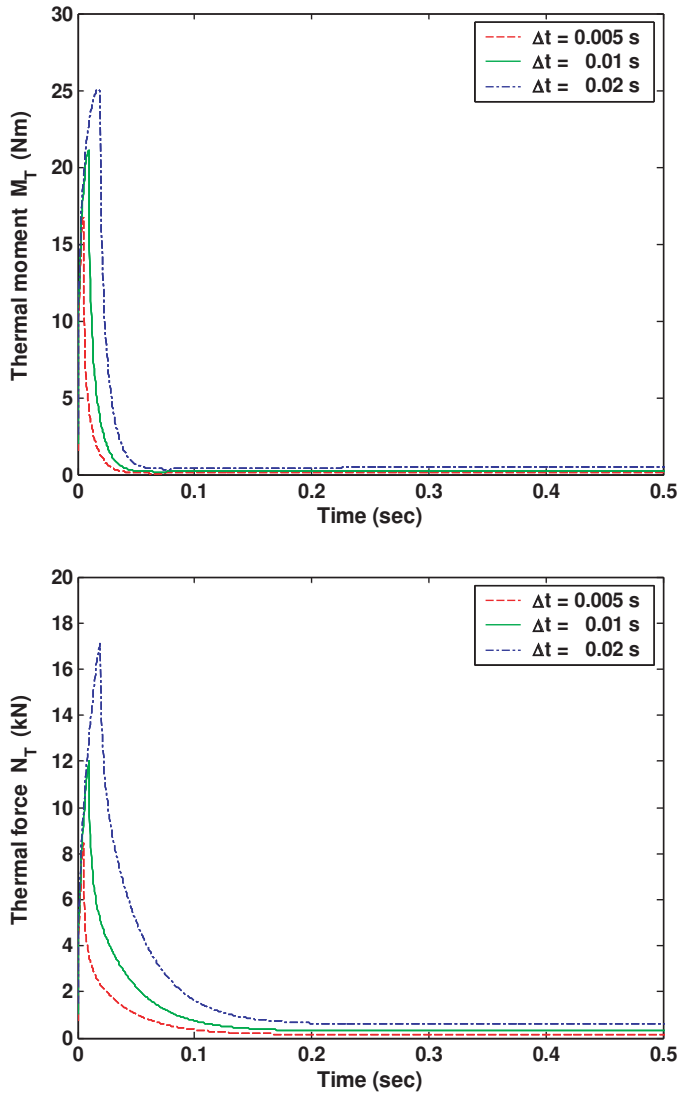
Figure 14. Time histories of the thermal moment M_T and thermal force N_T in the region $L_1 \leq x \leq (L - L_2)$ versus duration of thermal load Δt when $c = 4$ m/s.

Figure 14 shows the time histories of the thermal moments M_T and thermal forces N_T in the region $L_1 \leq x \leq (L - L_2)$ for different durations of thermal load, Δt, and Figure 15 shows the corresponding axial and transverse displacements. In general, it is shown that the amplitudes of vibration become larger as the duration of thermal load becomes larger.
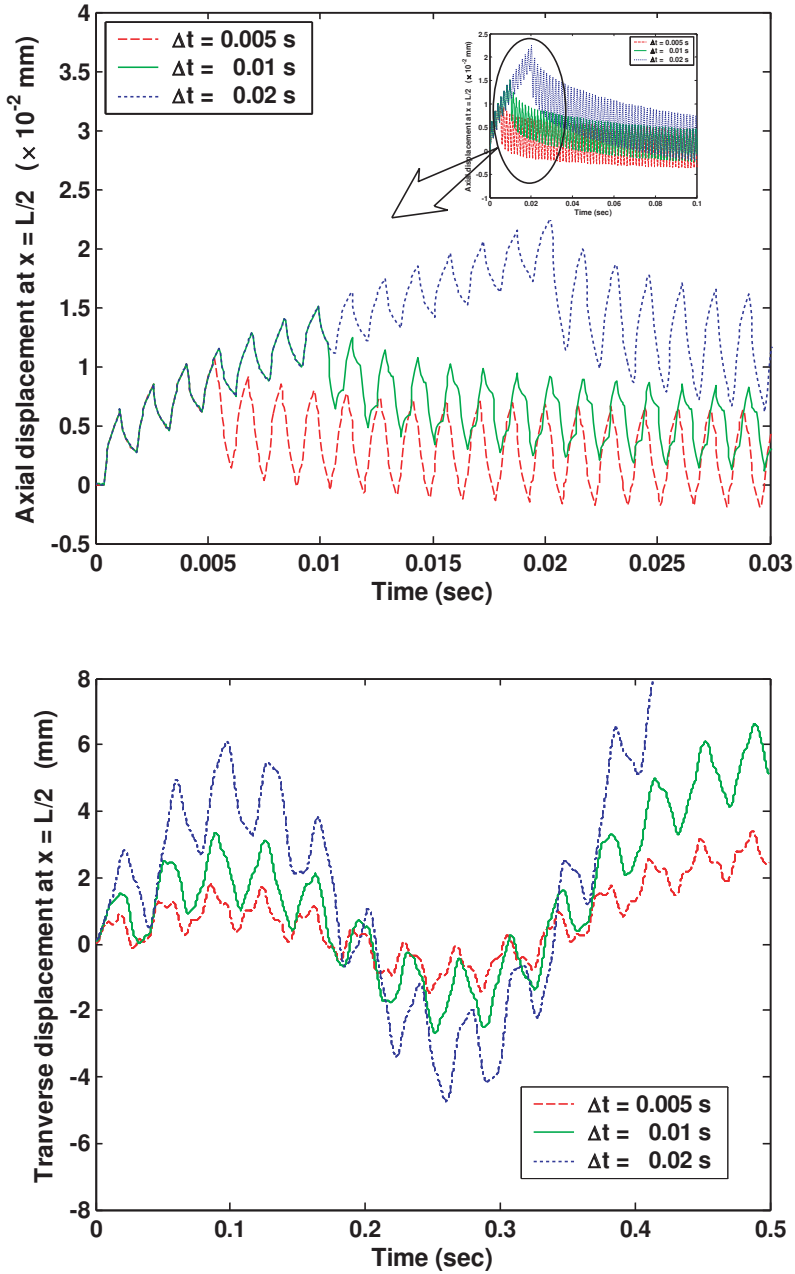
Figure 15. Time responses of axial and transverse displacements versus duration of thermal load Δt when $c = 4$ m/s.

5. Conclusions

We develop a spectral element model for an axially moving beam-plate subjected to external thermal loads. The model is formulated from frequency-dependent dynamic shape functions that are exact frequency-domain solutions of governing equations, and it is evaluated by comparison with the conventional finite element model. Numerical studies show the high accuracy of the present method and allow us to model the thermally induced vibration of an axially moving beam-plate subjected to a sudden temperature change on the upper surface of the beam-plate.

Appendix

Matrices $[S_{Un}]$ ***and*** $[S_{Wn}]$ ***in Equation*** (34).

$$[S_{Un}] = [X_n^{-1}]^T [R_{Un}][X_n^{-1}], \quad \text{where} \quad [R_{Un}] = \begin{bmatrix} Y_{n11} & 0 & 0 & Y_{n14} & 0 & 0 \\ 0 & 0 & 0 & 0 & 0 & 0 \\ 0 & 0 & 0 & 0 & 0 & 0 \\ Y_{n14} & 0 & 0 & Y_{n44} & 0 & 0 \\ 0 & 0 & 0 & 0 & 0 & 0 \\ 0 & 0 & 0 & 0 & 0 & 0 \end{bmatrix} \quad \text{and}$$

$$Y_{nij} = \frac{e^{(k_{ni}+k_{nj})l} - 1}{k_{ni} + k_{nj}} (\overline{EA} k_{ni} k_{nj} - \rho A \omega_n^2).$$

$$[S_{Wn}] = [X_n^{-1}]^T [R_{Wn}][X_n^{-1}], \quad \text{where} \quad [R_{Wn}] = \begin{bmatrix} 0 & 0 & 0 & 0 & 0 & 0 \\ 0 & X_{n11} & X_{n12} & 0 & X_{n13} & X_{n14} \\ 0 & X_{n12} & X_{n22} & 0 & X_{n23} & X_{n24} \\ 0 & 0 & 0 & 0 & 0 & 0 \\ 0 & X_{n13} & X_{n23} & 0 & X_{n33} & X_{n34} \\ 0 & X_{n14} & X_{n24} & 0 & X_{n34} & X_{n44} \end{bmatrix}$$

and $X_{nij} = \dfrac{e^{(\lambda_{ni}+\lambda_{nj})l} - 1}{\lambda_{ni} + \lambda_{nj}} \left(D\lambda_{ni}^2 \lambda_{nj}^2 - R_n \lambda_{ni} \lambda_{nj} + i\rho A c \omega_n (\lambda_{ni} - \lambda_{nj}) - \rho A \omega_n^2 \right).$

The finite element model

The finite element model used in this study is formulated by assuming the displacement fields within a finite beam-plate element of length l as follows:

$$u(x, t) = [N_U(x)]\{d(t)\}, \qquad w(x, t) = [N_W(x)]\{d(t)\},$$

where $\{d(t)\}$ is the nodal DOF vector defined by

$$\{d(t)\} = \left\{ u_1(t) \ \ w_1(t) \ \ \phi_1(t) \ \ u_2(t) \ \ w_2(t) \ \ \phi_2(t) \right\}^T$$

and $[N_U(t)]$ and $[N_W(t)]$ are the shape function matrices defined by

$$[N_U(x)] = \begin{bmatrix} 1 - \xi & 0 & 0 & \xi & 0 & 0 \end{bmatrix} \quad \text{and} \quad [N_W(x)] = \begin{bmatrix} 0 & N_{W1} & N_{W2} & 0 & N_{W3} & N_{W4} \end{bmatrix},$$

where $\xi = x/l$ and

$$N_{W1} = 2\xi^3 - 3\xi^2 + 1, \quad N_{W2} = l\xi(\xi-1)^2, \quad N_{W3} = -2\xi^3 + 3\xi^2, \quad N_{W4} = l\xi(\xi^2-\xi).$$

Following the usual procedure [Reddy 2002], the finite element equation can be derived as

$$[M]\{\ddot{d}\} + [C]\{\ddot{d}\} + [K]\{d\} = \{f\},$$

where $\{f\}$ is the nodal force vector defined by

$$\{f\} = \left\{ N_1 - N_T/2 \quad V_1 \quad M_1 + M_T/2 \quad N_2 + N_T/2 \quad V_2 \quad M_2 - M_T/2^T \right\}$$

$$+ \int_0^l \left(p_x[N_U]^T + p_z[N_W]^T \right) dx$$

and the finite element matrices $[M]$, $[C]$, and $[K]$ are given by

$$[M] = \int_0^l \left(\rho A[N_U]^T[N_U] + \rho A[N_W]^T[N_W] - \rho I[N_W']^T[N_W'] \right) dx$$

$$= \frac{\rho Al}{420} \begin{bmatrix} 140 & 0 & 0 & 70 & 0 & 0 \\ 0 & 156 & 22l & 0 & 54 & -13l \\ 0 & 22l & 4l^2 & 0 & 13l & -3l^2 \\ 70 & 0 & 0 & 140 & 0 & 0 \\ 0 & 54 & 13l & 0 & 156 & -22l \\ 0 & -13l & -3l^2 & 0 & -22l & 4l^2 \end{bmatrix} - \frac{\rho I}{30l} \begin{bmatrix} 0 & 0 & 0 & 0 & 0 & 0 \\ 0 & 36 & 3l & 0 & -36 & 3l \\ 0 & 3l & 4l^2 & 0 & -3l & l^2 \\ 0 & 0 & 0 & 0 & 0 & 0 \\ 0 & -36 & -3l & 0 & 36 & -3l \\ 0 & 3l & -l^2 & 0 & -3l & 4l^2 \end{bmatrix}$$

$$[C] =$$

$$\int_0^l \left(\rho Ac([N_W]^T[N_W'] - [N_W']^T[N_W]) \right) dx = \frac{\rho Ac}{30} \begin{bmatrix} 0 & 0 & 0 & 0 & 0 & 0 \\ 0 & 0 & 6l & 0 & 30 & -6l \\ 0 & -6l & 0 & 0 & 6l & -l^2 \\ 0 & 0 & 0 & 0 & 0 & 0 \\ 0 & -30 & -6l & 0 & 0 & 6l \\ 0 & 6l & l^2 & 0 & -6l & 0 \end{bmatrix}$$

$$[K] = \int_0^l \left(\overline{EA}[N_U']^T[N_U'] + D[N_W'']^T[N_W''] + \rho Ac^2[N_W']^T[N_W'] \right) dx$$

$$= \frac{\overline{EA}}{l} \begin{bmatrix} 1 & 0 & 0 & -1 & 0 & 0 \\ 0 & 0 & 0 & 0 & 0 & 0 \\ 0 & 0 & 0 & 0 & 0 & 0 \\ -1 & 0 & 0 & 1 & 0 & 0 \\ 0 & 0 & 0 & 0 & 0 & 0 \\ 0 & 0 & 0 & 0 & 0 & 0 \end{bmatrix} + \frac{D}{l^3} \begin{bmatrix} 0 & 0 & 0 & 0 & 0 & 0 \\ 0 & 12 & 6l & 0 & -12 & 6l \\ 0 & 6l & 4l^2 & 0 & -6l & 2l^2 \\ 0 & 0 & 0 & 0 & 0 & 0 \\ 0 & -12 & -6l & 0 & 12 & -6l \\ 0 & 6l & 2l^2 & 0 & -6l & 4l^2 \end{bmatrix} -$$

$$-\frac{\rho A c^2}{30l}\begin{bmatrix} 0 & 0 & 0 & 0 & 0 & 0 \\ 0 & 36 & 3l & 0 & -36 & 3l \\ 0 & 3l & 4l^2 & 0 & -3l & -l^2 \\ 0 & 0 & 0 & 0 & 0 & 0 \\ 0 & -36 & -3l & 0 & 36 & -3l \\ 0 & 3l & -l^2 & 0 & -3l & 4l^2 \end{bmatrix}.$$

References

[Al-Huniti 2004] N. S. Al-Huniti, "Dynamic behavior of a laminated beam under the effect of a moving heat source", *J. Compos. Mater.* **38**:23 (2004), 2143–2160.

[Arafat et al. 2003] H. N. Arafat, W. Faris, and A. H. Nayfeh, "Vibrations and buckling of annular and circular plates subjected to a thermal load", in *44th AIAA/ASME/ASCE/AHS Structures, Structural Dynamics, and Materials Conference* (Norfolk, VA, 2003), AIAA, 2003.

[Beck and McMasters 2004] J. V. Beck and R. L. McMasters, "Solutions for multi-dimensional transient heat conduction with solid body motion", *Int. J. Heat Mass Transf.* **47**:17–18 (2004), 3757–3768.

[Biot 1956] M. Biot, "Thermoelasticity and irreversible thermodynamics", *J. Appl. Phys.* **27** (1956), 240–253.

[Blevins 1979] R. D. Blevins, *Formulas for natural frequency and mode shape*, Van Nostrand Reinhold, New York, 1979.

[Boley 1956] B. A. Boley, "Thermally induced vibrations of beams", *J. Aeronaut. Sci.* **23** (1956), 179–181.

[Boley and Barber 1957] B. A. Boley and A. D. Barber, "Dynamic response of beams and plates to rapid heating", *J. Appl. Mech.* (*Trans. ASME*) **24** (1957), 413–416.

[Chandrashekhara and Tenneti 1994] K. Chandrashekhara and R. Tenneti, "Non-linear static and dynamic analysis of heated laminated plates: a finite element approach", *Compos. Sci. Technol.* **51**:1 (1994), 85–94.

[Eslami and Vahedi 1989] M. R. Eslami and H. Vahedi, "Coupled thermoelasticity beam problems", *AIAA J.* **27**:5 (1989), 662–665.

[Kidawa-Kukla 1997] J. Kidawa-Kukla, "Vibration of a beam induced by harmonic motion of a heat source", *J. Sound Vib.* **205**:2 (1997), 213–222.

[Kinra and Milligan 1994] V. K. Kinra and K. B. Milligan, "A second-law analysis of thermoelastic damping", *J. Appl. Mech.* (*Trans. ASME*) **61** (1994), 71–76.

[Kozlov 1972] V. Kozlov, "Thermoelastic vibrations of a rectangular plate", *Prikl. Mat. Mekh* **8** (1972), 123–127.

[Lee 1985] U. Lee, "Thermoelastic and electromagnetic damping analysis", *AIAA J.* **23**:11 (1985), 1783–1790.

[Lee 2004] U. Lee, *Spectral element method in structural dynamics*, Inha University Press, Incheon, Korea, 2004.

[Lee and Leung 2000] U. Lee and A. Y. T. Leung, "The spectral element method in structural dynamics", *Shock Vibr. Dig.* **32**:6 (2000), 451–465.

[Lord and Shulman 1967] H. Lord and Y. Shulman, "A generalized dynamical theory of thermoelasticty", *J. Mech. Phys. Solids* **15**:5 (1967), 299–309.

[Manolis and Beskos 1980] G. D. Manolis and D. E. Beskos, "Thermally induced vibrations of beam structures", *Comput. Methods Appl. Mech. Eng.* **21**:3 (1980), 337–355.

[Massalas and Kalpakidis 1984] C. V. Massalas and V. K. Kalpakidis, "Coupled thermoelastic vibrations of a Timoshenko beam", *Lett. Appl. Eng. Sci.* **22**:4 (1984), 459–465.

[Massalas et al. 1982] C. V. Massalas, A. Dalamangas, and G. Tzivanidis, "A note on the dynamics of thermoelastic thin plates", *J. Sound Vib.* **81**:2 (1982), 303–306.

[Mukherjee and Sinha 1996] N. Mukherjee and P. K. Sinha, "Thermal shocks in composite plates: a coupled thermoelastic finite element analysis", *Compos. Struct.* **34**:1 (1996), 1–12.

[Newland 1993] D. E. Newland, *Random vibrations, spectral and wavelet analysis*, 3 ed., Longman, New York, 1993.

[Oguamanam et al. 2004] D. C. D. Oguamanam, J. S. Hansen, and G. R. Heppler, "Nonlinear transient response of thermally loaded laminated panels", *J. Appl. Mech.* (*Trans. ASME*) **71**:1 (2004), 49–56.

[Özisik 1993] M. N. Özisik, *Heat conduction*, 2 ed., Wiley, New York, 1993.

[Reddy 2002] J. N. Reddy, *Energy principles and variational methods in applied mechanics*, Wiley, Hoboken, 2002.

[Sharma 2001] J. N. Sharma, "Three-dimensional vibration analysis of a homogeneous transversely isotropic thermoelastic cylindrical panel", *J. Acoust. Soc. Am.* **110**:1 (2001), 254–259.

[Takeuti and Furukawa 1981] Y. Takeuti and T. Furukawa, "Some considerations on thermal shock problems in a plate", *J. Appl. Mech.* (*Trans. ASME*) **48**:2 (1981), 113–118.

[Takeuti et al. 1983] Y. Takeuti, R. Ishida, and Y. Tanigawa, "On an axisymmetric coupled thermal stress problem in a finite circular cylinder", *J. Appl. Mech.* (*Trans. ASME*) **50** (1983), 116–121.

[Tauchert 1991] T. R. Tauchert, "Thermally induced flexure, buckling, and vibration of plates", *Appl. Mech. Rev.* **44**:8 (1991), 347–360.

[Thornton 1992] E. A. Thornton, "Thermal structures: four decades of progress", *J. Aircr.* **29**:3 (1992), 485–498.

[Trajkovski and Čukić 1999] D. Trajkovski and R. Čukić, "A coupled problem of thermoelastic vibrations of a circular plate with exact boundary conditions", *Mech. Res. Commun.* **26**:2 (1999), 217–224.

[Ugral 1999] A. C. Ugral, *Stresses in plates and shells*, McGraw-Hill, New York, 1999.

[Verma 2001] K. L. Verma, "Thermoelastic vibrations of a transversely isotropic plate with thermal relaxations", *Int. J. Solids Struct.* **38**:46–47 (2001), 8529–8546.

[Yu 1969] Y. Y. Yu, "Thermally induced vibration and flutter of a flexible boom", *J. Spacecr. Rockets* **6**:8 (1969), 902–910.

KYUNGSOO KWON: g2041021@inhaian.net
Department of Mechanical Engineering, Inha University, 253 Yonghyun-Dong, Nam-Ku, Incheon 402-751, Korea

USIK LEE: ulee@inha.ac.kr
Department of Mechanical Engineering, Inha University, 253 Yonghyun-Dong, Nam-Ku, Incheon 402-751, Korea